

# Signatures of Natural Selection in a Primate Bitter Taste Receptor

Stephen Wooding

Received: 10 August 2011 / Accepted: 14 December 2011 / Published online: 5 January 2012  
© Springer Science+Business Media, LLC 2012

**Abstract** Bitter taste receptors (TAS2Rs) enable animals to detect and avoid toxins in the environment, including noxious defense compounds produced by plants. This suggests that TAS2Rs are under complex pressures from natural selection. To investigate these pressures, we examined signatures of selection in the primate *TAS2R38* gene. Whole-gene (1,002 bp) sequences from 40 species representing all major primate taxa uncovered extensive variation. Nucleotide substitutions occurred at 448 positions, resulting in 201 amino acid changes. Two single-nucleotide deletions, one three-nucleotide in-frame deletion, and one premature stop codon were also observed. The rate of non-synonymous substitution ( $\omega = dN/dS$ ), was high in *TAS2R38* ( $\omega = 0.60$ ) compared to other genes, but significantly lower than expected under neutrality ( $P = 4.0 \times 10^{-9}$ ), indicating that purifying selection has maintained the basic structure of the receptor. However, differences were present among receptor subregions. Non-synonymous rates were significantly lower than expected in transmembrane domains ( $\omega = 0.55$ ,  $P = 1.18 \times 10^{-12}$ ) and internal loops ( $\omega = 0.51$ ,  $P = 7.04 \times 10^{-5}$ ), but not external loops ( $\omega = 1.16$ ,  $P = 0.53$ ), and evidence of positive selection was found in external loop 2, which exhibited a high rate ( $\omega = 2.53$ ) consistent with rapid shifts in ligand targeting. These patterns point to a history of rapid yet constrained change in bitter taste responses in the course of primate evolution.

DNA sequences analyzed in this study are deposited in GenBank with IDs JQ272198–JQ272237.

S. Wooding (✉)  
McDermott Center for Human Growth and Development,  
University of Texas Southwestern Medical Center, 6000 Harry  
Hines Boulevard, Dallas, TX 75390-8591, USA  
e-mail: stephen.wooding@utsouthwestern.edu

**Keywords** Bitter · TAS2R · Receptor · Primate · Selection

## Introduction

In mammals, bitter taste perception is initiated by G protein-coupled receptors (GPCRs) encoded by the *TAS2R* gene family, which are expressed in taste bud cells on the surface of the tongue and soft palate (Adler et al. 2000; Chandrashekar et al. 2000; Hoon et al. 1999). When exposed to their agonists, TAS2Rs trigger a downstream transductional cascade, producing a neural signal. TAS2Rs are capable of responding to a wide variety of natural and synthetic compounds, including numerous toxins utilized by plants to deter herbivores (Meyerhof et al. 2010). For instance, TAS2R7 responds to strychnine (found in plants in the genus *Strychnos*) (Sainz et al. 2007), TAS2R14 responds to noscapine (found in *Papaver* spp.) (Behrens et al. 2004), and TAS2R16 responds to salicin (*Salix* spp.) (Bufe et al. 2002). The responsiveness of TAS2Rs to plant toxins, together with the importance of plants as a source of nutrition in most animal diets, suggests that the evolution of bitter taste perception has been strongly driven by the need of herbivores to regulate toxin exposure.

Patterns of genetic and genomic variation indicate that natural selection has played an important role in the evolution of *TAS2Rs*. For example, in mammals, the number of active *TAS2R* loci ranges from ~10 to 40, while the *TAS1R* family, which encodes receptors initiating sweet and umami (savory) tastes, is encoded by just three loci (Shi et al. 2003). In addition, recently duplicated *TAS2Rs* show signs of rapid divergence in structural regions involved in ligand recognition (Shi and Zhang 2006). These patterns suggest that *TAS2Rs* as a family have been

pressured to diversify, to enable animals to perceive a broad range of bitter substances (Shi et al. 2003). However, evidence of selective effects varies both among taxa and among genes. For instance, while cross-gene comparisons indicate that selective pressures on *TAS2Rs* are relaxed in higher primates, population genetic analyses have found signatures of balancing and positive selection at some loci in humans (Fischer et al. 2005; Kim et al. 2005; Parry et al. 2004; Soranzo et al. 2005; Wang et al. 2004; Wooding et al. 2004).

To explore the role of natural selection in shaping diversity at an individual *TAS2R* locus across species, we examined patterns of variation at *TAS2R38* in primates. In humans, *TAS2R38* encodes a receptor responsive to natural and synthetic thyroid inhibitors including isothiocyanates (ITCs, found in plants in the Brassicaceae family), phenylthiocarbamide (PTC), and propylthiouracil (PROP/PTU), a drug used to treat hyperthyroidism (Kim et al. 2003; Meyerhof et al. 2010; Wooding et al. 2010). Many non-human primates exhibit ability to perceive PTC as well, suggesting that *TAS2R38*'s functionality has been conserved in the course of primate evolution (Chiarelli 1963; Eaton and Gavan 1965). However, PTC perception is not retained across all species and three, human (*Homo sapiens*), chimpanzee (*Pan troglodytes*), and Japanese macaque (*Macaca fuscata*), exhibit within-species polymorphism in sensitivity as the result of mutations in *TAS2R38* (Kim et al. 2003; Suzuki et al. 2011; Wooding et al. 2006). This suggests that functionality in *TAS2R38* may confer little fitness benefit, so evolutionary processes have been selectively neutral. To examine the evolutionary processes underlying these patterns, we analyzed genetic diversity in *TAS2R38* in 40 species, using phylogenetic analysis by maximum likelihood (PAML) to test for signatures of natural selection across the gene as a whole, in key structural landmarks, and among taxa.

## Methods

### Samples

Forty species representing all five major primate taxa were included in the study sample: Hominoidea (great apes;  $n = 9$  species), Cercopithecinae (i.e., baboons and macaques;  $n = 13$ ), Ceboidea (New World monkeys;  $n = 8$ ), Colobinae (leaf-eating monkeys;  $n = 6$ ), Lemuriformes (prosimians;  $n = 3$ ), and a non-primate outgroup, northern tree shrew (*Tupaia belangeri*) (Table 1). DNA samples for most species were obtained from the Coriell Institute for Medical Research Integrated Primate Biomaterials and Information Resource (IPBIR; Camden, NJ, USA). The human (*H. sapiens*) and chimpanzee (*P. troglodytes*)

**Table 1** Sampled species

IPBIR ID	Species	Common name
<u>Apes</u>		
n/a*	<i>Homo sapiens</i>	Human
n/a*	<i>Pan troglodytes</i>	Chimpanzee
NG05253	<i>Pan paniscus</i>	Bonobo
NG05251	<i>Gorilla gorilla</i>	Gorilla
NA04272	<i>Pongo pygmaeus abelii</i>	Sumatran orangutan
NG05252	<i>Pongo pygmaeus pygmaeus</i>	Bornean orangutan
PR00243	<i>Hylobates pileatus</i>	Pileated gibbon
PR00495	<i>Hylobates lar</i>	Lar gibbon
PR00721	<i>Hylobates syndactylus</i>	Siamang
<u>Leaf-eating monkeys</u>		
PR00679	<i>Nasalis larvatus</i>	Proboscis monkey
PR00379	<i>Semnopithecus entellus</i>	Gray langur
PR01099	<i>Trachypithecus francoisi</i>	Francois's leaf monkey
PR00296	<i>Colobus angolensis</i>	Angolan colobus monkey
PR00980	<i>Colobus guereza</i>	Eastern black-and-white colobus
PR00597	<i>Colobus polykomos</i>	Western black-and-white colobus
<u>Cercopithecus</u>		
NG07109	<i>Macaca mulatta</i>	Rhesus monkey
NG07921	<i>Macaca nemestrina</i>	Pig-tailed macaque
NG07101	<i>Macaca nigra</i>	Celebes macaque
NA03443	<i>Macaca arctoides</i>	Stump-tailed macaque
PR00232	<i>Mandrillus leucophaeus</i>	Drill
PR00716	<i>Miopithecus talapoin</i>	Talapoin monkey
PR00486	<i>Cercopithecus wolfi</i>	Wolf's guenon
PR00283	<i>Cercopithecus lhoesti</i>	L'hoest's guenon
PR00566	<i>Cercopithecus ascanius</i>	Red-tail monkey
PR00762	<i>Cercopithecus petaurista</i>	Mona monkey
PR00198	<i>Allenopithecus nigroviridis</i>	Allen's swamp monkey
NG06116	<i>Erythrocebus patas</i>	Patas monkey
PR00990	<i>Chlorocebus aethiops</i>	Vervet
<u>New World monkeys</u>		
n/a†	<i>Callithrix jacchus</i>	Common marmoset
NG05308	<i>Saguinus labiatus</i>	Red-bellied tamarin
NG05313	<i>Saguinus fuscicollis</i>	Saddle-backed tamarin
NG05311	<i>Saimiri sciureus</i>	Common squirrel monkey
PR01143	<i>Aotus azarae</i>	Owl monkey
NG05356	<i>Lagothrix lagotricha</i>	Woolly monkey
NG05352	<i>Ateles geoffroyi</i>	Spider monkey
NG06115	<i>Callicebus moloch</i>	Dusky titi monkey
<u>Prosimians</u>		
NG07099	<i>Lemur catta</i>	Ring-tailed lemur
PR00275	<i>Microcebus murinus</i>	Mouse lemur
PR00049	<i>Otolemur garnettii</i>	Garnett's galago
n/a†	<i>Tupaia belangeri</i>	Northern tree shrew

Columns indicate the identification number, species designation, and common name in the IPBIR

\* Wooding laboratory sample

† Sequence obtained from published genome data

samples were sequenced in a previous study (Wooding et al. 2004). Common marmoset (*Callithrix jacchus*) and tree shrew (*T. belangeri*) sequences were obtained from whole-genome data published by the Washington University Genome Sequencing Center.

#### DNA Sequencing

DNA sequences were obtained from the entire coding region of *TAS2R38* gene (1,002 bp) in all samples. Initial primer sets for use in PCR amplification and sequencing were designed using aligned, published genome sequences from human (*H. sapiens*), chimpanzee (*P. troglodytes*), macaque (*Macaca mulatta*), common marmoset (*C. jacchus*), mouse lemur (*Microcebus murinus*), galago (*Otolemur garnettii*), and Northern tree shrew (*T. belangeri*), which were used to identify invariant annealing sites in flanking regions. PCR was performed using the Clontech Advantage-GC 2 PCR Kit (Clontech Laboratories, Inc., Mountain View, CA, USA). Sequencing was performed using standard capillary-based methods on ABI 3730 sequencing hardware.

#### Sequence Analysis

Sequences were aligned with the ClustalW (version 1.83) computer program using default settings, and phylogenetic relationships were determined using the neighbor-joining algorithm implemented in PHYLIP (version 3.65) (Felsenstein 2007). Substitutional saturation, which can result in erroneous parameter estimates and confound tests for natural selection, was evaluated using the method of Xia et al. (2003; Xia and Xie 2001), which compares an index of the information content of a set of sequences ( $I_{SS}$ ) with the critical value necessary for hypothesis testing ( $I_{SS,C}$ ).

#### Tests for Natural Selection

To determine whether signatures of natural selection were present, we analyzed relative rates of synonymous and non-synonymous substitution,  $\omega$  ( $=dN/dS$ ), which are shaped by long-term selective pressures. Under neutrality, relative rates of synonymous and non-synonymous change are expected to be equal, such that  $\omega = 1$ . In contrast, purifying selection preferentially removes non-synonymous variants from populations, suppressing  $\omega$  ( $<1$ ), while positive selection favors non-synonymous variants, shifting  $\omega$  upwards ( $>1$ ). Further, these trends can be localized, affecting only some gene sites or regions. We tested for these effects across *TAS2R38* as a whole and in regions encoding key functional categories and landmarks. These analyses excluded three species with altered stop codons, which are unsuitable for modeling  $\omega$ .

We analyzed  $\omega$  using the likelihood-based methods of Yang et al. (2005), which compare models of  $\omega$  under varying constraints. These analyses were performed using PAML version 4 software, which we used to estimate  $\omega$  and other parameters under seven models formulated by Yang et al. (2005): Model M0 (one  $\omega$ ) and Model M0 ( $\omega = 1$ ), in which  $\omega$  is allowed to take a single value across a gene; Model M1a (nearly neutral), in which sites fall into two categories, with  $\omega = 1$  in one category and  $\omega < 1$  estimated in the other; Model M2a (positive selection), in which three  $\omega$  categories are specified, with one constrained to  $\omega < 1$ , one fixed at  $\omega = 1$  and one constrained to  $\omega > 1$ ; Model M7 ( $\beta$ ), which specifies a parameter,  $\beta$ , describing a probability distribution of  $\omega$  values among sites; Model 8a ( $\beta$  &  $\omega = 1$ ), which specifies  $\beta$  along with a  $\omega$  value fixed at 1; and M8 ( $\beta$  &  $\omega$ ), which specifies both  $\beta$  and a category of sites with a separately estimated  $\omega > 1$  (Yang 2007).

Likelihood estimates obtained using PAML were used to perform tests for selection by comparing pairs of alternative models. To determine whether  $\omega$  was consistent with an overall absence of natural selection (i.e., neutrality) in *TAS2R38*, we compared the likelihood of Model M0 (one  $\omega$ ), in which  $\omega$  takes a single estimated value across a gene, and Model M0 ( $\omega = 1$ ), in which  $\omega$  is constrained to 1. In this test,  $\omega$  estimates significantly below 1 are consistent with the prevalence of purifying natural selection, which tends to remove non-synonymous variants, while estimates above 1 are consistent with positive natural selection, which favors non-synonymous variants. We also performed three tests for positive selection: M1a (nearly neutral) versus M2a (positive selection), M7 ( $\beta$ ) versus M8 ( $\beta$  &  $\omega$ ), and M8a ( $\beta$  &  $\omega = 1$ ) versus M8 ( $\beta$  &  $\omega$ ). To compensate for multiple testing, significance thresholds were corrected using the false discovery rate model of Benjamini and Hochberg (1995).

## Results and Discussion

### Genetic Variation

The basic architecture of the *TAS2R38* (1,002 bp, 333 aa) was retained across all but four species. Two species departed from this motif as the result of microdeletions. Woolly monkey (*Lagothrix lagotricha*) harbored a single-base deletion at nucleotide 977, resulting in a frameshift. The proximity of the mutation to the end of the gene results in a predicted translational stop 38 bp downstream of the normal stop, rather than a premature stop as is often the case with frameshifts. Thus, the expected result of the mutation is an alteration of the last eight amino acids of the gene along with the addition of 13 amino acids at the C

terminus. Spider monkey (*Ateles geoffroyi*) contained a CAG (glutamine) to TAG (stop) substitution at position 229 (aa 77), truncating the encoded receptor to ~25% of its typical length. Because altered stop codons are predicted to be highly disruptive to receptor function, these two taxa were excluded from further analysis. One species, Sumatran orangutan (*Pongo pygmaeus abelii*), exhibited a large number of heterozygous nucleotide positions including six non-synonymous variants and a single-base frameshift deletion, suggesting that *TAS2R38* may be duplicated. A third species, *T. belangeri* (northern tree shrew) included an in-frame 3 bp deletion at nucleotides 532–534, causing the deletion of an asparagine (N) at aa 178.

Across the 37 species with intact *TAS2R38* loci, 448 of 1,002 possible nucleotide positions (45%) were variable, resulting in variation at 201 of 333 amino acid positions (60%). Variable sites were distributed across the length of the receptor (Fig. 1). However, there was an enrichment of substitutions in external loops (ELs), which varied at 72% of positions (33 of 46). Fewer substitutions were observed in transmembrane regions (TMs), which varied at 56% (111 of 199), and internal loops (ILs), which varied at 65% (57 of 88). The presence of such large numbers of variable sites in sequence data is a potential sign of substitutional saturation, which can reduce information content, but tests using Xia and Xie's (2001) methods determined that

saturation levels were significantly lower than critical values necessary for phylogenetic analysis and selection tests ( $I_{ss} \sim 0.10$ ;  $I_{ss,c} \sim 0.80$ ;  $P < 1.0 \times 10^{-4}$ ).

A neighbor-joining tree based on aligned *TAS2R38* sequences from 39 of the 40 sampled species in our study, excluding Sumatran orangutan, was congruent with previously published phylogenies (Fig. 2) (Purvis 1995). The earliest divergence in the tree differentiated the prosimians from all other primates. Similarly, the New World monkeys were distinguished from the Old World monkeys and apes, and the Old World monkeys were appropriately divided into the leaf-eating (Colobine) monkeys and the Cercopithecine monkeys. Within-clade relationships were also consistent with previous phylogenetic estimates, although some topological differences involving closely related species were present. For instance, the tree inferred from *TAS2R38* grouped the genus *Mandrillus* with the genus *Cercopithecus* as opposed to *Macaca* (Purvis 1995).

## Signatures of Natural Selection

### Gene-Wide Signatures

Across *TAS2R38* as a whole,  $\omega$  was consistent with the presence of pervasive pressure from purifying natural selection. Fitting PAML Model M0 (one  $\omega$ ), in which  $\omega$  is the

**Fig. 1** Variable amino acid positions in the 37 species analyzed using PAML. Circles indicate the relative position of amino acids in the *TAS2R38* receptor from the N terminus (position 1) to the C terminus (position 333). External, transmembrane, and internal sites were categorized following Floriano et al. (2006). Filled circles indicate whether variation was present at the given position in the overall primate alignment (i.e., whether more than one amino acid was observed at the position). For each site category (external, transmembrane, internal), values at right indicate the number of sites in the category (denominator), the number of variable sites (numerator), and the fraction of variable sites (in parentheses)

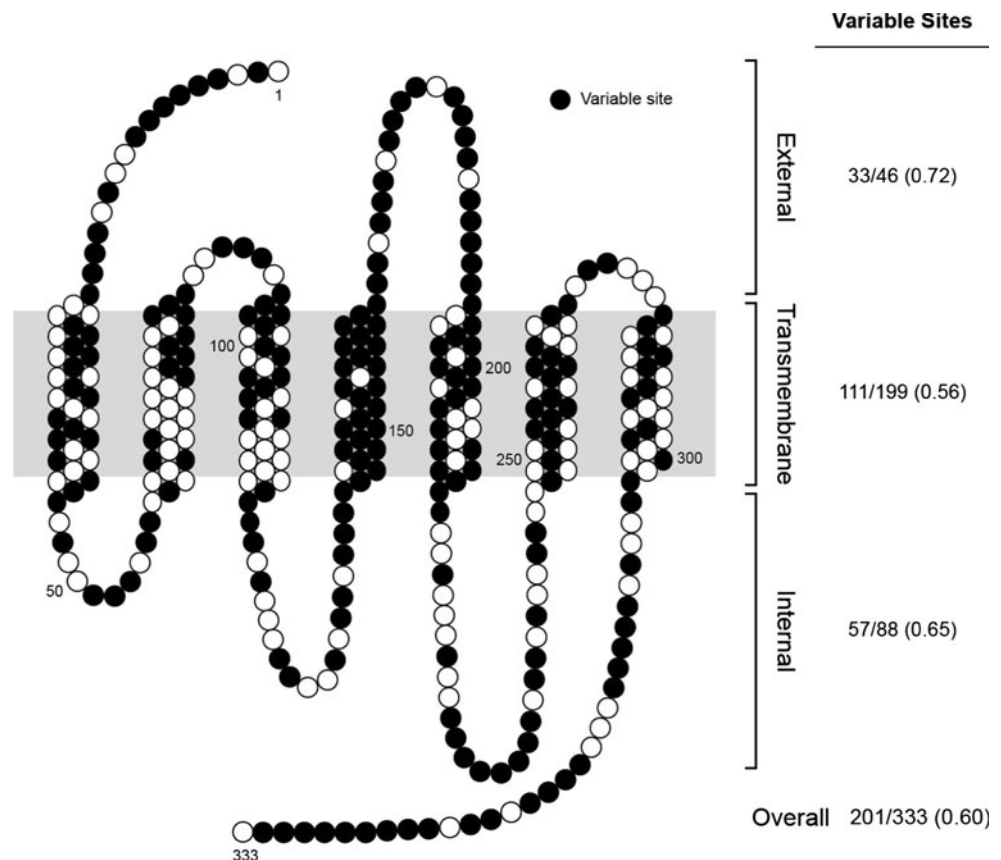
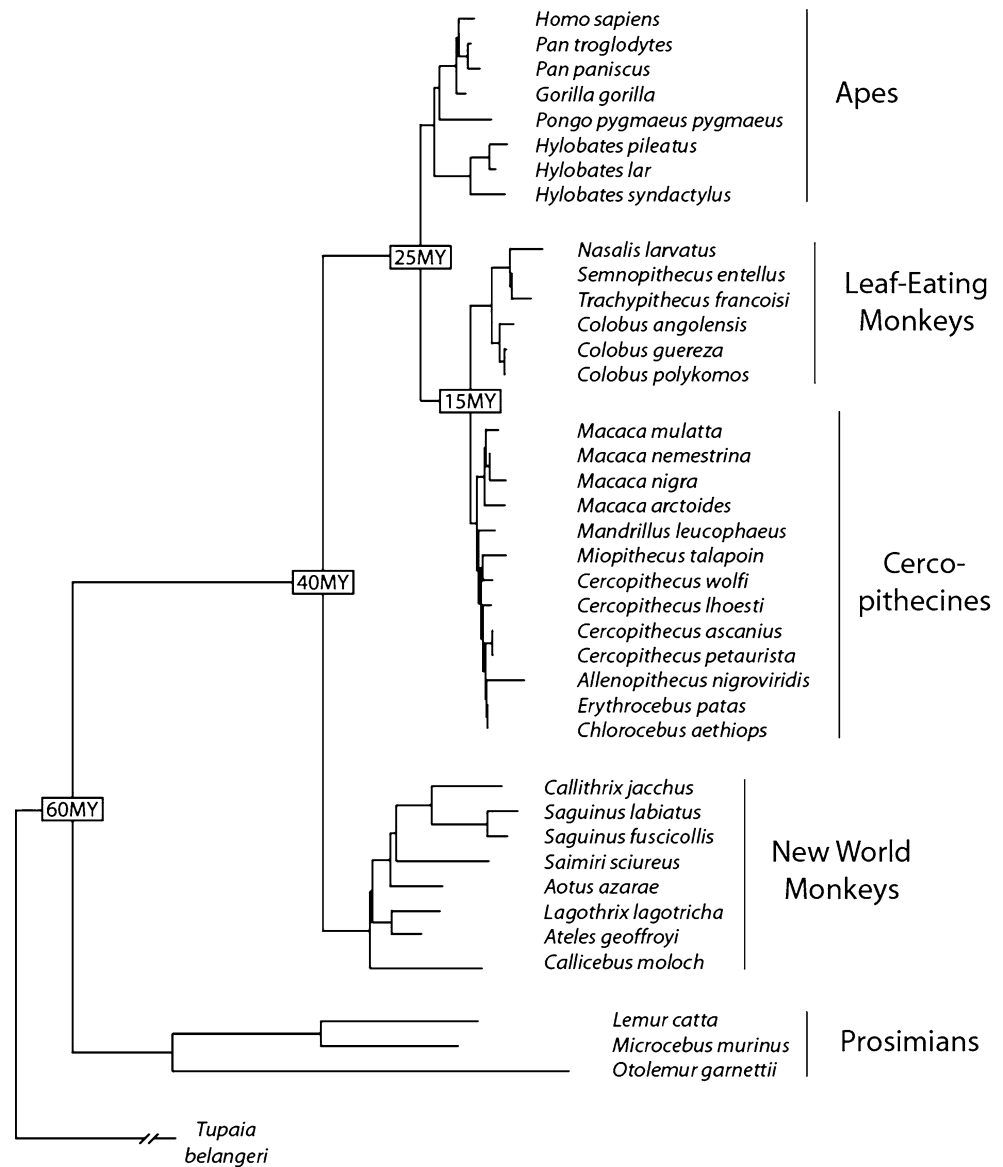


**Fig. 2** Neighbor-joining tree of *TAS2R38* sequences used in PAML analyses. Boxes indicate dates of divergence among clades, millions of years before present, estimated by Purvis (1995)



sole free parameter, yielded an estimate of  $\omega = 0.60$  with a log likelihood ( $\ln L$ ) of  $-5020.68$  (Table 2A). This estimate is far higher than in most genes examined to date. Toll-Riera et al. (2011), for instance, obtained a mean estimate of  $\omega = 0.14$  across  $\sim 3,000$  genes. Thus, amino acid substitutions have accumulated in *TAS2R38* at a relatively high rate in primates. However, the fit of Model 0 with  $\omega$  fixed at one, the expectation under neutrality, had a far lower log likelihood than did Model 0 (one  $\omega$ ),  $-5038.35$ . Thus, the estimated value of  $\omega$ , while high, was significantly lower than expected under neutrality ( $2dL = 35.34$ ,  $df = 1$ ;  $P = 2.77 \times 10^{-9}$ ) (Table 2A). This finding strongly contradicts the hypothesis that *TAS2R38* has been evolving neutrally.

Evidence that purifying selection has been a pervasive force in the overall evolution of a gene does not rule out the importance of other selective pressures. Variation in selective pressure often arises among sites and regions as

the result of differences in functional constraint. For instance,  $\omega$  estimates in the mammalian DRB gene, which participates in MHC-II-mediated immune responses, are consistent with overall pressure from purifying selection; however, regions involved in antigen recognition show signatures of positive selection (Furlong and Yang 2008). Shi et al. (2003) found similar patterns in a study of divergence among *TAS2R* loci in humans. In *TAS2Rs*, non-synonymous rates in TMs and internal loops were significantly below 1 ( $\omega = 0.46$  and  $0.51$ ), consistent with purifying selection, while rates in ELs, which participate in ligand recognition, were near one ( $\omega = 1.06$ ), consistent with neutrality. Further, Shi et al. (2003) found five specific amino acid positions in ELs showing evidence of positive selection (aa 16, 177, 253, 254, and 268).

To determine whether signatures of positive selection were present in our sample, we performed three model

**Table 2** PAML analyses across all sites and species

A				
Model	In <i>L</i>	Estimates		
M0 ( $\omega = 1$ )	−5.038.35	n/a		
M0 (one $\omega$ )	−2020.68	$\hat{\omega} = 0.60$		
M0 ( $\omega$ free)	−4991.18	n/a		
M1a (nearly neutral)	−4994.07	$\hat{p}_0 = 0.50$ ( $\hat{p}_1 = 0.50$ ). $\hat{\omega}_0 = 0.18$ ( $\hat{\omega}_1 = 1$ )		
M2a (positive selection)	−4991.46	$\hat{p}_0 = 0.52$ , $\hat{p}_1 = 0.43$ ( $\hat{p}_2 = 0.05$ ) $\hat{\omega}_0 = 0.21$ , ( $\hat{\omega}_1 = 1$ ) $\hat{\omega}_2 = 2.20$		
M7 ( $\beta$ )	−4995.10	$\hat{p} = 0.43$ , $\hat{q} = 0.31$		
M7 ( $\beta$ & $\omega = 1$ )	−4992.94	$\hat{p} = 0.50$ , ( $\hat{p}_1 = 0.50$ ), $\hat{p}_1 = 0.34$ $\hat{q} = 0.99$ , ( $\hat{\omega} = 1.0$ )		
M8 ( $\beta$ & $\omega$ )	−4991.35	$\hat{p}_0 = 0.83$ , ( $\hat{p}_1 = 0.17$ ), $\hat{p} = 0.98$ $\hat{q} = 1.27$ , $\hat{\omega} = 1.60$		
B				
Tests	2dL	df	<i>p</i>	
Neutrality				
M0 (One $\omega$ ) vs. M0 ( $\omega = 1$ )	35.54	1	$2.77 \times 10^{-9}$ **	
Positive selection				
M1a (nearly neutral) vs. M2a (positive selection)	5.22	2	0.07	
M7 ( $\beta$ ) vs. M8 ( $\beta$ & $\omega = 1$ )	6.90	2	0.03	
M7 ( $\beta$ & $\omega = 1$ ) vs. M8 ( $\beta$ & $\omega$ )	2.58	1	0.11	

A—Random-sites models, likelihoods, and parameter estimates. For each model, two parameter types are shown,  $\omega$  and  $P$ . Each  $\omega$  value indicates a dN/dS estimate. For models with more than one site class, each of which has a separate  $\omega_i$ , the frequency of sites in each class is  $p_i$ . Un-subscripted  $P$  and  $q$  values indicate parameters of  $\beta$  distributions. B—Model comparisons testing for departures from neutrality and positive selection

\*\* $p < 0.01$

comparisons: Model M1a (nearly neutral) versus M2a (positive selection) and M7 ( $\beta$ ) versus M8 ( $\beta$  &  $\omega$ ), and M8a ( $\beta$  &  $\omega = 1$ ) versus M8 ( $\beta$  &  $\omega$ ) (Table 2B). Fitting Model M2a to our data suggested that a small proportion of sites (0.05) with  $\omega > 1$  is present, which is potentially consistent with the effects of localized positive selection. However, the fit was not significantly better than that of Model M1a, and the nearly neutral model was not rejected (ln *L* −4991.46 vs. −4994.07;  $P = 0.07$ ). Fitting Model M8 also indicated that sites with  $\omega > 1$  may be present but, again, the enrichment of high  $\omega$  sites was not statistically significant relative to expectations under either Model 7 or model M8a when multiple testing was taken into account (ln *L* −5093.91 vs. −5095.91,  $P = 0.03$ ; ln *L* −4992.94 vs. −4991.65,  $P = 0.11$ ). In addition, no specific sites showing evidence of positive selection were identified under M2a or M8. Taken together, these results indicate that if *TAS2R38* harbors positions with elevated  $\omega$  values, the number of positions involved must be low, the  $\omega$  elevation modest, or both.

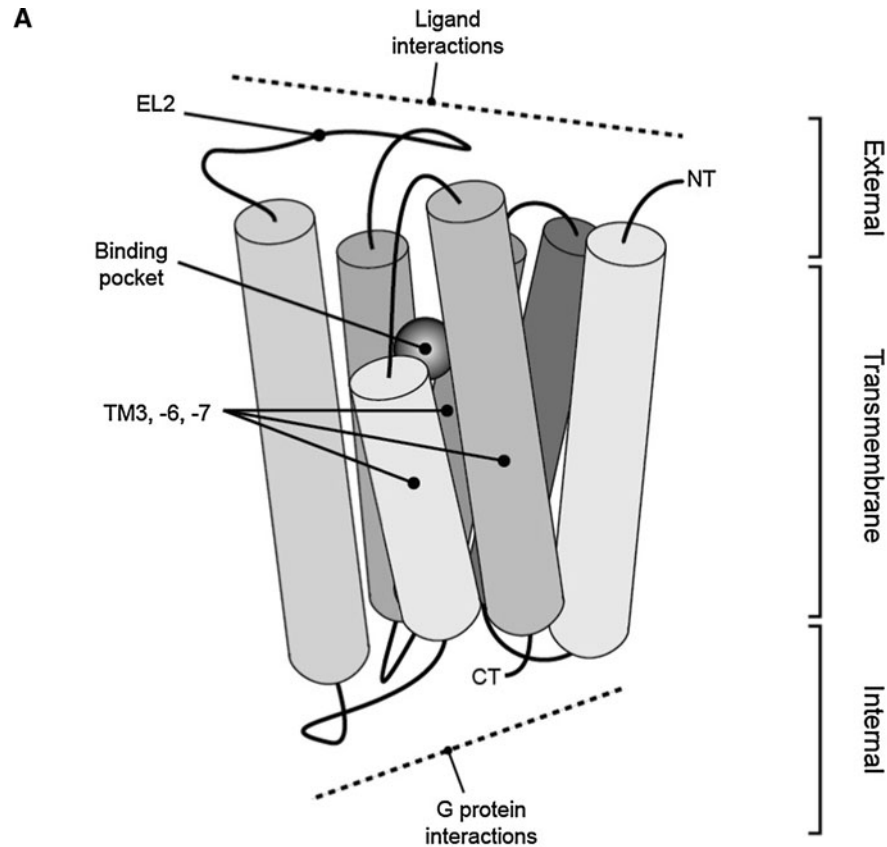
### Structure-Specific Signatures

GPCRs as family share a conserved underlying structure with three primary functional categories: ELs, which mediate extracellular ligand interactions; TMs, which are important to both receptor orientation and ligand binding, and internal loops (ILs), which mediate intracellular

interactions with G proteins (Vaidehi et al. 2002) (Fig. 3a). This organization has led to the long-held hypothesis that ELs, TMs, and ILs are under different selective pressures, with ELs being labile and TMs and ILs constrained (Strotmann et al. 2011). To examine this prediction in *TAS2R38*, we tested for signatures of selection in each functional category.

Signatures of selection in functional categories were consistent with general predictions for GPCRs (Fig. 3b). While  $\omega$  in ELs was slightly above one and did not differ from neutral expectations ( $\omega = 1.16$ ,  $P = 0.53$ ), estimates in TMs and internal loops were below 1 with a high level of significance ( $\omega = 0.55$ ,  $P = 1.18 \times 10^{-12}$ ;  $\omega = 0.51$ ,  $P = 4.76 \times 10^{-5}$ ), a signature of purifying selection. These estimates are strikingly similar to those obtained by Shi et al. (2003) in their study of inter-gene divergence in *TAS2Rs*: 1.06, 0.46, and 0.51, respectively. Both results are consistent with the hypothesis that natural selection has acted to preserve regions essential to the basic functionality of *TAS2R38* while regions involved in ligand interactions have evolved more quickly. Nonetheless, while  $\omega$  estimates were high, particularly in ELs, tests for positive selection under models M2a and M8 detected no significant enrichment of high  $\omega$  sites in any of the three functional categories. Thus, while regions broadly hypothesized to participate in ligand interactions did show high rates of substitution relative to other parts of the receptor, they did not show definitive evidence of rapid, ongoing adaptation.

**Fig. 3** Functional landmarks and structure-specific tests for neutrality. **a** Predicted secondary structure and functional landmarks in TAS2R38 proposed by Floriano et al. (2006). **b** Likelihoods, parameter estimates, and *p* values obtained for each structure independently under Model 0 ( $\omega = 1$ ) and Model 0 (one  $\omega$ )



<b>B Structure</b>	<b>lnL (<math>\omega = 1</math>)</b>	<b>lnL (one <math>\omega</math>)</b>	<b><math>\hat{\omega}</math></b>	<b>2dL</b>	<b><i>p</i> (df = 1)</b>
External	-742.36	-742.16	1.16	0.40	0.53
Transmembrane	-2939.83	-2914.57	0.55	50.52	$1.18 \times 10^{-12}$ *
Internal	-1305.21	-1296.93	0.51	16.54	$4.76 \times 10^{-5}$ *
TM3, -6, -7	-1122.82	-1107.60	0.38	30.46	$3.41 \times 10^{-8}$ *
EL2	-300.95	-298.15	2.53	5.60	0.02*

*Signatures in Ligand-Binding Regions*

Beyond the broadly defined functional categories retained across GPCRs, two regions of TAS2R38 have been specifically identified as important in ligand recognition, suggesting that they may be under particularly strong selective pressure: TMs -3, -6, and -7, and EL2. Structure–function studies have demonstrated that TMs -3, -6, and -7 orient to form a binding pocket essential for agonist recognition (Fig. 3a) (Floriano et al. 2006; Vaidehi et al. 2002). However, they are also important in propagating the binding signal to intracellular regions interfaced with G proteins (Okada et al. 2001). The dual role of TMs -3, -6, and -7 suggests that they are under countervailing selective pressures: while their participation in ligand recognition suggests that they are under pressure to recognize potentially diverse compounds in the environment, their importance in propagating binding signals

suggests that they are constrained by the need to retain basic functionality. In contrast, EL2 is principally involved in extracellular interactions with agonists, and some evidence suggests that it participates directly in ligand binding (Ivanov et al. 2009; Palczewski et al. 2000; Vaidehi et al. 2002). This suggests that variation in EL2 is less constrained, and more likely to be influenced by pressures related to ligand recognition.

Tests for neutrality detected different levels of constraint in TM3, -6, -7 and EL2. Fitting Model M0 (one  $\omega$ ) to the TM3, -6, and -7 data indicated that these regions are conserved relative to other parts of the receptor (Fig. 3b). Their estimated  $\omega$  was substantially lower than across the gene overall ( $\omega = 0.38$  vs.  $\omega = 0.60$ ), and significantly lower than expected under neutrality ( $P = 3.41 \times 10^{-8}$ ), a strong signature of purifying selection. In contrast, fitting M0 (one  $\omega$ ) to the EL2 data yielded an estimate substantially higher than across TAS2R38 overall (2.53 vs. 0.60)

**Table 3** Tests for positive selection in EL2

Test	In $L$	Estimates	$P$	Selected sites (BEB)
M1a (nearly neutral) vs. M2a (positive selection)	–300.95 –297.74	$\hat{p}_o = 0.00$ ( $\hat{p}_1 = 1.00$ ) $\hat{\omega}_0 = 0.18$ ( $\hat{\omega}_1 = 1$ ) $\hat{p}_o = 0.16$ , $\hat{p}_1 = 0.57$ ( $\hat{p} = 0.26$ ) $\hat{\omega}_0 = 1.00$ , ( $\hat{\omega}_1 = 1$ ), $\hat{\omega}_2 = 3.63$	0.04**	<b>166</b> , <i>183</i>
M7 ( $\beta$ ) vs. M8 ( $\beta$ & $\omega = 1$ )	–300.95 –297.74	$\hat{p} = 1.17$ , $\hat{q} = 0.01$ $\hat{p}_o = 0.43$ , ( $\hat{p}_1 = 0.57$ ), $\hat{p} = 14.16$ $\hat{q} = 0.01$ , $\hat{\omega} = 3.63$	0.04**	<b>166</b> , <i>173</i> , <b>183</b> , <b>186</b>
M7 ( $\beta$ & $\omega = 1$ ) vs. M8 ( $\beta$ & $\omega$ )	–300.59 –297.74	$\hat{p}_0 = 0.01$ , ( $\hat{p}_1 = 0.99$ ) $\hat{p} = 0.48$ $\hat{q} = 1.55$ , ( $\hat{\omega} = 1.00$ ) $\hat{p}_o = 0.43$ , ( $\hat{p}_1 = 0.57$ ) $\hat{p} = 14.16$ $\hat{q} = 0.01$ , $\hat{\omega} = 3.63$	0.02**	<b>166</b> , <i>173</i> , <b>183</b> , <b>186</b>

Models, likelihoods, and parameter estimates were obtained to perform three comparisons: M1a (nearly neutral) versus M2a (positive selection) and M7 ( $\beta$ ) versus M8 ( $\beta$  &  $\omega$ ). The rightmost column (selected sites) indicates positions departing from expectation at  $P = 0.01$  (bold) and 0.05 (italic) levels for each pair of models under Bayes–Empirical–Bayes estimates for individual sites

\*\* $p < 0.01$

and significantly greater than expected under neutrality ( $P = 0.02$ ), a sign of positive selection, even when multiple testing was taken into account. These patterns suggest that although both regions participate in ligand recognition, adaptive processes have prevailed in EL2, while TMs –3, –6, and –7 have been under negative pressure.

In addition to showing an overall signature of positive selection, EL2 exhibited some evidence of selection at specific sites. Maximum likelihood estimates under both M2a (positive selection) and M8 ( $\beta$  &  $\omega$ ) identified site categories with high  $\omega$  values ( $>3.5$ ), and M1a (nearly neutral) and M7 ( $\beta$ ) were both marginally rejected in favor of the models without high- $\omega$  categories (M1a,  $P = 0.04$ ; M7,  $P = 0.04$ ; M8a,  $P = 0.02$ ) (Table 3). Further, site-by-site estimates under M2a and M8 using the Bayes–Empirical–Bayes (BEB) methods of Yang et al. (2005) identified four positions with significantly elevated  $\omega$  values (sites 166, 173, 183, and 186), suggesting that they may be particularly important to adaptive processes in *TAS2R38* (Table 3). Three of these sites (positions 166, 183, and 186) harbored changes affecting hydrophobicity, a type of substitution that often results in altered receptor function. One (186) also harbored a variant affecting charge. The fourth, 173, harbored only hydrophobic residues.

## Conclusions

Signatures of natural selection across *TAS2R38* both as a unit and within structural and functional subregions point to a complex history of selective pressures in primates. Across *TAS2R38*, rates of non-synonymous substitution

were high, but still suppressed relative to neutral expectations, indicating that purifying selection has been a pervasive force in the evolution of *TAS2R38* in primates. This suggests that the integrity of the gene has been largely maintained throughout the course of primate evolution. The responsiveness of human *TAS2R38* to compounds synthesized by the plant family Brassicaceae, which is highly diverse ( $>3,700$  species) and has a worldwide distribution, suggests that selective constraints may have been exerted specifically by exposure to these plants. However, elevated non-synonymous rates in gene subregions responsible for ligand interactions indicates that substantial functional diversity is present. The presence of greatly elevated rates in EL2 in particular, which has been implicated as a direct participant in ligand recognition, suggests that the range of compounds to which *TAS2R38* is responsive has shifted over time (Palczewski et al. 2000; Vaidehi et al. 2002).

Patterns of variation in our sample raise numerous questions about selective trends in the *TAS2R* family as a whole. A notable pattern in our data was that substitution rates in regions encoding ELs, TMs, and ILs in primate *TAS2R38* ( $\omega = 1.16$ , 0.55, and 0.51) were similar to rates estimated in cross-gene comparisons of human *TAS2R* loci ( $\omega = 1.06$ , 0.46, and 0.51) (Shi et al. 2003). This suggests that patterns of divergence in *TAS2R38* are typical of *TAS2Rs* as a family. However, it does not imply that selective pressures are identical among loci. Within humans, different *TAS2Rs* respond to different compound repertoires; thus, variation in selective pressure is likely. For instance, it could be that selective pressures on *TAS2Rs* targeted at toxins present in the diet of primates' ancestors, but not primates themselves, are relaxed.



Dissecting these patterns by examining and comparing multiple loci will shed light on the evolutionary challenges of bitter taste perception on both an organismal and a molecular level.

## References

- Adler E, Hoon MA, Mueller KL, Chandrashekar J, Ryba NJ, Zuker CS (2000) A novel family of mammalian taste receptors. *Cell* 100:693–702
- Behrens M, Brockhoff A, Kuhn C, Bufe B, Winnig M, Meyerhof W (2004) The human taste receptor hTAS2R14 responds to a variety of different bitter compounds. *Biochem Biophys Res Commun* 319:479–485
- Benjamini Y, Hochberg Y (1995) Controlling the false discovery rate: a practical and powerful approach to multiple testing. *J R Stat Soc Ser B* 57:289–300
- Bufe B, Hofmann T, Krautwurst D, Raguse JD, Meyerhof W (2002) The human TAS2R16 receptor mediates bitter taste in response to beta-glucopyranosides. *Nat Genet* 32:397–401
- Chandrashekar J, Mueller KL, Hoon MA, Adler E, Feng L, Guo W, Zuker CS, Ryba NJ (2000) T2Rs function as bitter taste receptors. *Cell* 100:703–711
- Chiarelli B (1963) Sensitivity to P.T.C. (phenyl-thio-carbamide) in primates. *Folia Primatol* 1:73–87
- Eaton JW, Gavan JA (1965) Sensitivity to P-T-C among primates. *Am J Phys Anthropol* 23:381–388
- Felsenstein J (2007) PHYLIP (Phylogeny Inference Package) version 3.65. Distributed by the author. Department of Genome Sciences, University of Washington, Seattle
- Fischer A, Gilad Y, Man O, Pääbo S (2005) Evolution of bitter taste receptors in humans and apes. *Mol Biol Evol* 22:432–436
- Floriano W, Hall S, Vaidehi N, Kim U, Drayna D, Goddard W (2006) Modeling the human PTC bitter-taste receptor interactions with bitter tastants. *J Mol Model* 12:931–941
- Furlong RF, Yang Z (2008) Diversifying and purifying selection in the peptide binding region of DRB in mammals. *J Mol Evol* 66:384–394
- Hoon MA, Adler E, Lindemeier J, Battey JF, Ryba NJ, Zuker CS (1999) Putative mammalian taste receptors: a class of taste-specific GPCRs with distinct topographic selectivity. *Cell* 96:541–551
- Ivanov AA, Barak D, Jacobson KA (2009) Evaluation of homology modeling of G-protein-coupled receptors in light of the A(2A) adenosine receptor crystallographic structure. *J Med Chem* 52:3284–3294
- Kim UK, Jorgenson E, Coon H, Leppert M, Risch N, Drayna D (2003) Positional cloning of the human quantitative trait locus underlying taste sensitivity to phenylthiocarbamide. *Science* 299:1221–1225
- Kim U, Wooding S, Ricci D, Jorde LB, Drayna D (2005) Worldwide haplotype diversity and coding sequence variation at human bitter taste receptor loci. *Hum Mutat* 26:199–204
- Meyerhof W, Batram C, Kuhn C, Brockhoff A, Chudoba E, Bufe B, Appendino G, Behrens M (2010) The molecular receptive ranges of human TAS2R bitter taste receptors. *Chem Senses* 35:157–170
- Okada T, Ernst OP, Palczewski K, Hofmann KP (2001) Activation of rhodopsin: new insights from structural and biochemical studies. *Trends Biochem Sci* 26:318–324
- Palczewski K, Kumasaka T, Hori T, Behnke CA, Motoshima H, Fox BA, Le Trong I, Teller DC, Okada T, Stenkamp RE, Yamamoto M, Miyano M (2000) Crystal structure of rhodopsin: A G protein-coupled receptor. *Science* 289:739–745
- Parry CM, Erkner A, le Coutre J (2004) Divergence of T2R chemosensory receptor families in humans, bonobos, and chimpanzees. *Proc Natl Acad Sci USA* 101:14830–14834
- Purvis A (1995) A composite estimate of primate phylogeny. *Philos Trans R Soc Lond B Biol Sci* 348:405–421
- Sainz E, Cavenagh M, Gutierrez J, Battey J, Northup J, Sullivan S (2007) Functional characterization of human bitter taste receptors. *Biochem J* 403:537–543
- Shi P, Zhang J (2006) Contrasting modes of evolution between vertebrate sweet/umami receptor genes and bitter receptor genes. *Mol Biol Evol* 23:292–300
- Shi P, Zhang J, Yang H, Zhang YP (2003) Adaptive diversification of bitter taste receptor genes in Mammalian evolution. *Mol Biol Evol* 20:805–814
- Soranzo N, Bufe B, Sabeti PC, Wilson JF, Weale ME, Marguerie R, Meyerhof W, Goldstein DB (2005) Positive selection on a high-sensitivity allele of the human bitter-taste receptor TAS2R16. *Curr Biol* 15:1257–1265
- Strotmann R, Schrock K, Boselt I, Staubert C, Russ A, Schoneberg T (2011) Evolution of GPCR: change and continuity. *Mol Cell Endocrinol* 331:170–178
- Suzuki N, Sugawara T, Matsui A, Go Y, Hirai H, Imai H (2011) Identification of non-taster Japanese macaques for a specific bitter taste. *Primates* 51:285–289
- Toll-Riera M, Laurie S, Alba MM (2011) Lineage-specific variation in intensity of natural selection in mammals. *Mol Biol Evol* 28:383–398
- Vaidehi N, Floriano WB, Trabanino R, Hall SE, Freddolino P, Choi EJ, Zamanakos G, Goddard WA (2002) Prediction of structure and function of G protein-coupled receptors. *Proc Natl Acad Sci USA* 99:12622–12627
- Wang X, Thomas SD, Zhang J (2004) Relaxation of selective constraint and loss of function in the evolution of human bitter taste receptor genes. *Hum Mol Genet* 13:2671–2678
- Wooding S, Kim UK, Bamshad MJ, Larsen J, Jorde LB, Drayna D (2004) Natural selection and molecular evolution in PTC, a bitter-taste receptor gene. *Am J Hum Genet* 74:637–646
- Wooding S, Bufe B, Grassi C, Howard M, Stone A, Vazquez M, Dunn D, Meyerhof W, Weiss R, Bamshad M (2006) Independent evolution of bitter-taste sensitivity in humans and chimpanzees. *Nature* 440:930–934
- Wooding S, Gunn H, Ramos P, Thalmann S, Meyerhof W (2010) Genetics and bitter taste responses to goitrin, a plant toxin found in vegetables. *Chem Senses* 35:685–692
- Xia X, Xie Z (2001) DAMBE: software package for data analysis in molecular biology and evolution. *J Hered* 92:371
- Xia X, Xie Z, Salemi M, Chen L, Wang Y (2003) An index of substitution saturation and its application. *Mol Phylogenet Evol* 26:1
- Yang Z (2007) PAML 4: phylogenetic Analysis by Maximum Likelihood. *Mol Biol Evol* 24:1586
- Yang Z, Wong W, Nielsen R (2005) Bayes empirical bayes inference of amino acid sites under positive selection. *Mol Biol Evol* 22:1107–1118